UDK: 533.6:629.7.02.004:004.4
COSATI: 01-01

Software development for subsonic aircraft's longitudinal stability derivatives calculation

Nikola Maričić, PhD (Eng)[1)]

Longitudinal aerodynamic stability derivatives of subsonic general configuration aircraft can be calculated using finite element methodology based on the Doublet Lattice Method (DLM), the Slender Body Theory (SBT) and the Method of Images (MI). Applying this methodology, software DERIV is developed. The results obtained using this program is compared to NASTRAN examples HA21A and HA75H. A good agreement is achieved between results from DERIV, NASTRAN, [5] and [6].

Key words: **aerodynamics, unsteady aerodynamics, aerodynamic derivatives, longitudinal stability, subsonic aircraft.**

Introduction

DURING the 60s, as the computer aerodynamics was just starting to develop, the idea to make use of the lifting surfaces theories for estimation of aerodynamic derivatives was proposed [1]. All theories assume the linear-small amplitude, sinusoidal motion.

To the present day, especially for aircraft flutter clearance, a lot of methods have been developed for accuracy of steady and oscillatory aerodynamic loads determination. Nowadays these loads of general configuration are calculated using the vortex and doublet-lattice finite elements' methods. The chord wise and span wise load distribution on lifting surfaces and longitudinal (*z*-vertical and *y*-lateral) load distribution on bodies can be calculated for configurations that consist of an assemblage of lifting surfaces (with arbitrary plan form and dihedral, with or without control surfaces) and bodies (with variable circular or elliptic cross sections).

The numerical method used was in the paper developed for reliable calculation of flutter speeds of the subsonic aircraft. For, already known normal modes of the aircraft structure the unsteady, aerodynamic load distributions on general configuration can be calculated. This possibility can be used to calculate steady and unsteady aircraft stability aerodynamic derivations. In this case, input data comprise a few of special rigid body motions of aircraft structure. Choosing which rigid body motions depends whether longitudinal or lateral aircraft's aerodynamic derivatives are observed. In this paper, longitudinal derivatives are analyzed.

The software package UNAD, for calculation of subsonic, unsteady aerodynamic forces of general configuration, needed for flutter calculation was developed. The respective package has been modified and package DERIV developed for steady and unsteady longitudinal aerodynamic derivative calculation for subsonic, general configurations. The developed software DERIV was tested on NASTRAN examples HA21A and HA75H. The obtained results were compared to the data from NASTRAN, [5] and [6].

S&MN projecting teams for estimation of unsteady aerodynamic derivatives of general configuration use semi empirical method based on NASA's DATCOM software. Software DERIV is the first domestic package that can give steady and unsteady derivatives based on the integration of unsteady aerodynamic loads over the whole subsonic aircraft configuration.

Subsonic, unsteady aerodynamic loads

Aerodynamic finite element methods are based on a matrix equation:

$$\{w\} = [A]\{\Delta Cp\}\,,\ \Delta Cp = \frac{p_{lower} - p_{upper}}{\rho U^2 / 2} \qquad (1)$$

In eq.(1) $\{w\}$ is column matrix of downwashes (positive down), $[A]$ is square matrix of aerodynamic influence coefficients, and $\{\Delta Cp\}$ is column matrix of dimensionless lifting surface coefficients . The main flow is defined by density ρ and speed U of free stream. Aerodynamic elements are defined by general configuration geometry in the Cartesian coordinate system. The motion of general configuration is defined by degrees of freedom at aerodynamic grid points. Aerodynamic elements are trapezoidal boxes representing the lifting surfaces, ring slender bodies' elements, and ring image elements representing slender body and interference influence.

The DLM is used for interfering lifting surfaces in subsonic flow. As DLM is based on small-disturbance, linear aerodynamics, all lifting surfaces are assumed to lie nearly parallel to the main flow. Each interfering surface is divided into boxes. Boxes are small thick less (flat palate) trapezoidal lifting elements. The boxes are arranged to form

[1)] Faculty of Technical Sciences, 38220 Kosovska Mitrovica

strips. Strips lay parallel to free stream and the surface edges. Fold and hinge lines lie on the box boundaries. In order to reduce the number of variables, symmetry option is used. Unknown pressure ΔCp on each box is represented by a line of pressure doublet at quarter chord of the box. Known downwash w collocation (control) point lies at the mid span of the box three quarter chords. DLM aerodynamic elements are represented of Fig.1.

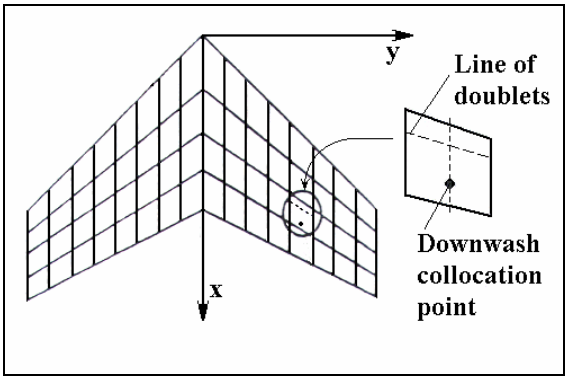

Figure 1. Lifting surface's idealization

SBT is used to determine lifting characteristics for isolated bodies. SBT assumes that the flow in the body vicinity is quasi-steady and two-dimensional. Bodies can have z-vertical, y-lateral or both degrees of freedom. Slender bodies of general configuration are divided slender body elements (axial velocity doublets) as shown on Fig.2. Slender body elements are used for calculating aerodynamic loading due to the motion of the body.

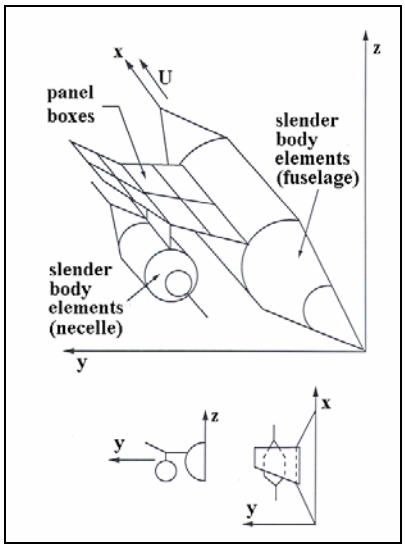

Figure 2. Idealization of slender body

The subsonic wing-body interference is based on the superposition of singularities and their images, described in the method of images (MI). Each slender body is substituted by cylindrical interference body, which circumscribes the slender body. The interference body is divided into interference elements, as shown on Fig.3. The interference element is used to include the influence of the other bodies and lifting surfaces on the body, to which the element belongs into calculation. Each interference element is substituted by *z*-vertical and *y*-lateral modified acceleration potential pressure doublets. The primary wing-body interference is accounted for by a system of images of DLM vortices and a system of doublets within each interference element. There is no influence between two interference elements which belong to the same interference body.

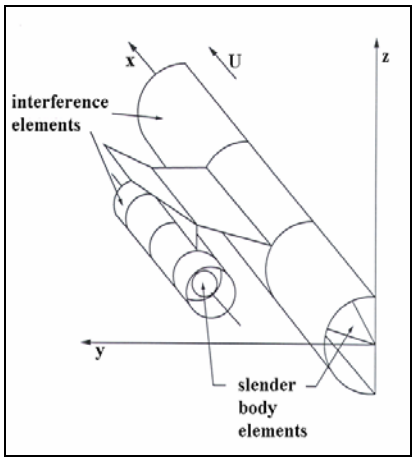

Figure 3. Interference element's idealization

The above taken into consideration, matrix eq. (1) can be written in the following form:

$$\begin{Bmatrix} \overline{w}_w \\ 0 \\ \overline{w}_s \end{Bmatrix} = \begin{bmatrix} A_{w,w} & A_{w,i} & A_{w,s} \\ A_{i,w} & A_{i,i} & A_{i,s} \\ 0 & 0 & A_{s,s} \end{bmatrix} \begin{Bmatrix} \Delta Cp \\ \mu_i \\ \mu_s \end{Bmatrix} \tag{2}$$

In eq. (2):

- $A_{r,s}$ is aerodynamic influence matrix element, which defines a part of normal wash on s-th finite element due to the unit strength r-th singularity. Indexes for the singularities and the aerodynamic finite elements are: w-lifting surface, i-image and s-slender body.
- $\overline{w}_w$ is the column of the known downwashes on the lifting surface elements in the collocation (control) points normalized by free stream speed U.
- $\overline{w}_i = \{0\}$ is the column of zero downwashes on the image elements.
- $\overline{w}_s$ is the column of the known downwashes on the slender body elements in axis midpoints normalized by free stream speed U.
- ΔCp is the unknown column of the strengths of lifting surface singularities (acceleration potential pressure doublets).
- μ_i is the unknown column of the strengths of images singularities (modified acceleration potential pressure doublets).
- μ_s is the known column of the strengths of slender body singularities (velocity potential doublets).

The strength of slender body velocity potential doublet of unit the length is known from the two-dimensional theory. For j-th slender body element, described by midpoint (ξ,η,ζ) and radius R_j, follows:

$$\mu_{s,j}(\xi,\eta,\zeta,\omega) = 2\pi R_j^2 U \overline{w}_{s,j}(\xi,\eta,\zeta,\omega)$$

In the above relation ω is the angular frequency of the harmonic motion of the slender body. As each slender body has *z*-vertical, *y*-lateral or both degrees of freedom, generally each j-th element of the body is substituted by the two

velocity potential doublets, acting on the real element's axial length $\Delta\xi_j$:

$$\mu_{s,j}^{(y)} = 2\pi R_j^2 U \bar{w}_{s,j}^{(y)} \ \Delta\xi_j \ ; \ \mu_{s,j}^{(z)} = 2\pi R_j^2 U \bar{w}_{s,j}^{(z)} \ \Delta\xi_j \quad (3)$$

If boundary values on slender bodies are known, the strength of the slender bodies' singularities can be calculated using eq. (3). Substituting these obtained strengths in eq. (2), it follows:

$$\begin{Bmatrix} \bar{w}_w - \Delta\bar{w}_w \\ -\Delta\bar{w}_i \end{Bmatrix} = \begin{bmatrix} A_{w,w} & A_{w,i} \\ A_{i,w} & A_{i,i} \end{bmatrix} \begin{Bmatrix} \Delta Cp \\ \mu_i \end{Bmatrix} \quad (4)$$

In eq. (4), $\bar{w}_w - \Delta\bar{w}_w$ and $-\Delta\bar{w}_i$ are modifications of normalized downwashes on lifting surface elements and images caused by the known slender body singularities. Eq. (4) represents a system of linear equations with complex coefficients. The system can be solved in terms of the known boundary conditions for the unknown ΔCp, $\mu_i^{(y)}$ and $\mu_i^{(z)}$.

Lifting surface pressure distribution ΔCp can be integrated to give the lifting surface contributions to the aerodynamic parameters of interest (aerodynamic coefficients, generalized forces, etc.).

The forces on the bodies are determined in a more complicated manner. Every lifting surface box ΔCp, every image $\mu_i^{(y)}$ and $\mu_i^{(z)}$, every slender body axis doublet $\mu_s^{(y)}$ and $\mu_s^{(z)}$ affects the force distribution on bodies. It is known from unsteady computational aerodynamics that every singularity can be obtained from the point pressure doublet whose normal wash flow field is obtained from the standard lifting surfaces kernel K. Pressure coefficient $Cp(x,y,z)$ at point (x,y,z) on the body surface due to point pressure doublet of the strength $\Delta Cp(\xi,\eta,\zeta)\ \Delta A$ in point (ξ,η,ζ) can be obtained by relation:

$$Cp(x,y,z) = \frac{\Delta Cp(\xi,\eta,\zeta)\Delta A}{4\pi} \ e^{\imath\lambda Ma(x-\xi)} \ \frac{\partial}{\partial N}\left(\frac{e^{-\imath\lambda R}}{R}\right) \quad (5)$$

In the above equation:

- Ma is free stream Mach number,
- $R^2 = (x-\xi)^2 + (1-Ma^2)\left[(y-\eta)^2 + (z-\zeta)^2\right]$,
- $\lambda = \dfrac{\omega Ma}{U(1-Ma^2)}$,
- $\vec{N}$ is the unit vector in the direction of the doublet.

The term $\Delta Cp(\xi,\eta,\zeta)\ \Delta A$ is the total pressure doublet strength of lifting surface box of area ΔA in which lifting pressure coefficient is $\Delta Cp(\xi,\eta,\zeta)$. An equivalent point pressure doublet is assumed to act in $\frac{1}{4}$-mid chord box's point of lifting surface element. The finite length of body doublet $\Delta\xi$ is obtained by two point pressure doublets per each body element. The first is located at the leading edge of the element and has the strength $\mu e^{\frac{\imath\omega\Delta\xi}{2U}}$, and the second at the trailing edge of the strength $-\mu e^{-\frac{\imath\omega\Delta\xi}{2U}}$.

Eq. (5) must be integrated over the whole body surface to the obtain forces acting on the body due to point doublet located at (ξ,η,ζ). Then the effects of all point pressure doublets must be summed to obtain total forces on the body. Integration of body force is given in [2] in detail.

Longitudinal derivatives

Generally, aircraft lift C_z and pitch moment C_m coeficients can be represented by the Mac Laurent series:

$$C_z = C_{z0} + C_{z\alpha}\alpha + C_{z\dot{\alpha}}\frac{\dot{\alpha}l}{2U} + C_{zq}\frac{\dot{\theta}l}{2U} + C_{z\ddot{\alpha}}\frac{\ddot{\alpha}l}{4U^2} + \\ + C_{z\dot{q}}\frac{\ddot{\theta}l}{4U^2} + \sum_{all\ controls}\left(C_{z\delta}\delta + C_{z\dot{\delta}}\frac{\dot{\delta}l}{2U} + \ldots\right) + \ldots \quad (6)$$

$$C_m = C_{m0} + C_{m\alpha}\alpha + C_{m\dot{\alpha}}\frac{\dot{\alpha}l}{2U} + C_{mq}\frac{\dot{\theta}l}{2U} + C_{m\ddot{\alpha}}\frac{\ddot{\alpha}l}{4U^2} + \\ + C_{m\dot{q}}\frac{\ddot{\theta}l}{4U^2} + \sum_{all\ controls}\left(C_{m\delta}\delta + C_{m\dot{\delta}}\frac{\dot{\delta}l}{2U} + \ldots\right) + \ldots \quad (7)$$

In (6) and (7), α is aircraft angle of attack, q is aircraft pitch velocity ($q = \dot{\theta}$), where θ is pitch angle over aircraft's center of gravity (cg) and l is reference length, usually mean wing aerodynamic chord l_{mac}. The total reference angle of attack α_m can be obtained as a linear combination of all kinematic effects involved:

$$\alpha_m = \alpha_{m0} + \alpha_{m\alpha}\alpha + \sum_{all\ controls}\alpha_{m\delta}\delta + \alpha_{mq}\frac{ql}{2U} + \alpha_{m\dot{\alpha}}\frac{\dot{\alpha}l}{2U} + \\ + \sum_{all\ controls}\alpha_{m\dot{\delta}}\frac{\dot{\delta}l}{2U} + \alpha_{m\ddot{\alpha}}\frac{\ddot{\alpha}l^2}{4U^2} + \alpha_{m\ddot{\theta}}\frac{\ddot{\theta}l^2}{4U^2} + \ldots$$

Based on relations (6) and (7), in aircraft control theory longitudinal aerodynamic derivatives can usually be divided into:

- steady longitudinal derivatives $\Rightarrow$ $C_{z\alpha}$, $C_{m\alpha}$, C_{zq}, C_{mq},
- unsteady longitudinal derivatives $\Rightarrow$ $C_{z\dot{\alpha}}$, $C_{m\dot{\alpha}}$, $C_{z\dot{q}}$, $C_{m\dot{q}}$, $C_{z\ddot{\alpha}}$, $C_{m\ddot{\alpha}}$.

In eqs. (6) and (7), the influences of slat deflections δ_{slat}, flap deflections δ_{flap}, symmetrical aileron deflections δ_{ail}^{symm}, elevator deflections δ_{elev} and symmetrical rudder deflections δ_{rudd}^{symm} (if fins are positioned out of aircraft symmetry plane) can be incorporated especially for calculation of the steady longitudinal derivatives. It should be mentioned that the aerodynamic forces on control surfaces strongly depend on their boundary layers. As in the used methods viscosity effects are neglected, derivatives with respect to δ and $\dot{\delta}$ will give only trends to accurate values.

The steady coefficients C_{z0} and C_{m0} are the aerodynamic coefficients for zero angle of attack ($\alpha = 0$). They are usually determined apart from longitudinal dynamic analysis. Values of these coefficients are dominantly influenced by viscousity effects and certainly determined on the wind tunnel tests. Of course, one can use semi-empirical methods or CFD programs (for $\alpha = 0$) to evaluate C_{z0} and C_{m0}, but obtained results are not reliable in many cases. However, for classical general configurations the coeffi-

cients C_{z0} and C_{m0} are small relative to the other parts in (6) and (7), so their influence can be neglected.

Generally speaking, aerodynamic stability derivatives are determined in $X_sY_sZ_s$ stability axis system, while aerodynamic forces and moments are calculated in aerodynamic axis system $X_aY_aZ_a$. The aerodynamic system is colinear with the velocity coordinate system $X_vY_vZ_v$. The axises of aerodynamic system are opposite to the axises of velocity system $(x_a=-x_v;\ y_a=-y_v;\ z_a=-z_v)$, when the motion of aircraft is in a straight line. All of the three systems have the same origin in the center of gravity C_{cg} of aircraft structure. All the above mentioned coordinate systems are represented in Fig.4. In connection with relation (6), it is necessary to outline that $C_{z_s}=C_{z_v}=-C_{z_a}$.

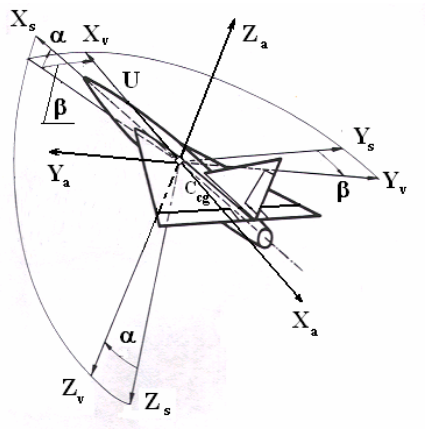

Figure 4. Used coordinate systems

In the reference condition the X_a - axis is parallel to airspeed U, but departs from it, X_s - axis is moving with the airplane during a disturbance. That means that the angle of attack α_s, defined as the angle between the X_s - axis and the direction of U, is not necessarily identical to absolute value of the angle of attack $\alpha_a=\alpha$, used in aerodynamic calculations. The axis X_a is in direction of the undisturbed flight path, while X_s - axis is oscillating with rigid airplane. Clearly, α_s represents the disturbance from an aerodynamic state α. As small disturbances have been assumed, simple conversion rules between the stability and the aerodynamic axis systems for symmetric motions are:

$$X_sY_sZ_s \Rightarrow\ -\alpha = ik\frac{h_z}{l_{mac}}+\theta \Leftarrow X_aY_aZ_a$$

$$X_sY_sZ_s \Rightarrow\ -q = ik\ \theta \qquad \Leftarrow X_aY_aZ_a$$

In the stability axis system α_s - variation is equivalent to a variation of down wash of the airplane. So, it is equivalent to the angle of attack to be prescribed in the methods used in this paper, where the aerodynamic axis system is used. A q -variation, as defined in the stability axis system, is felt by the airplane as linearly varying down wash in the aerodynamic system.

As it is said in the introduction of this paper, concept of integration of unsteady aerodynamic loads is used, so obtained lift $\bar{C}_z$ and pitch moment $\bar{C}_m$ coefficients are complex numbers. These complex coefficients are connected to (6) and (7) by relations:

$$C_z=\Re e\left(\bar{C}_z e^{\imath\omega t}\right);\ C_m=\Re e\left(\bar{C}_m e^{\imath\omega t}\right) \tag{8}$$

In order to calculate unsteady longitudinal derivatives, three general configuration motions are of interest. The first is quasi-steady harmonic change of attack angle, the second is slow steady pitch and the third is aircraft quasi-steady harmonic vertical translation:

A1. Quasi-steady harmonic change of the angle of attack $\Rightarrow(x,t)$; $\alpha_0=const.$

$$\alpha=\alpha_0 e^{\imath\omega\alpha}\Rightarrow\dot{\alpha}=\imath\omega\alpha\Rightarrow\ddot{\alpha}=-\omega^2\alpha\ ; \tag{9}$$

A2. Steady pitch angle $\Rightarrow\theta(x)$; $q=\frac{d\theta}{dt}=const.$

By introducing a constant pitch angular velocity q, it follows:

$$\theta=\frac{q(x-x_{cg})}{U}=\frac{ql_{mac}}{2U}\frac{2(x-x_{cg})}{l_{mac}}\equiv\frac{dh_{0p}}{dx} \tag{10}$$

For $\frac{ql_{mac}}{2U}=.1$ eq. (10) can be integrated:

$$\frac{dh_{0p}}{dx}=\frac{.2(x-x_{cg})}{l_{mac}}\Leftrightarrow h_{0p}=.1\frac{(x-x_{cg})^2}{l_{mac}} \tag{11}$$

It is clear that $dh_{0p}/dt=0$.

A3. Quasi-steady harmonic vertical translation $\Rightarrow h_z(t)$; $dh_z/dx=0$

$$h_z=h_{0z}e^{\imath\omega t}\Rightarrow\dot{h}_z=\imath\omega h_z\equiv\alpha_z U\Rightarrow\alpha_z=\imath\frac{\omega}{U}h_z=\imath\frac{k}{l_{mac}}h_z;\qquad k=\frac{\omega l_{mac}}{U} \tag{12}$$

Angle α_z is the angle of attack (from stability axis system) induced by quasi-steady, harmonic, vertical, small amplitude oscillations h_z relative to the path of aircraft motion. In the relation (12), k is reduced frequency.

As in the steady calculations harmonic vertical translation does not exist and vs. in the unsteady calculations steady pitch doesn't exist, the cases A2. and A3. can be treated as one case.

In the flutter calculation the boundary conditions can be obtained from the shapes of the normal modes of the aircraft structure (deflections and slopes of mode shape). In, for example [7], it is shown that the boundary condition – normalized downwash on each lifting surface or body's element is:

$$\bar{w}_{ij}=\frac{w_{ij}}{U}=\frac{dh_{0_j}}{dx}+\frac{1}{U}\frac{dh_{0_j}}{dt}=\frac{dh_{0_j}}{dx}+\imath\frac{\omega}{U}h_{0_j};\ ;\qquad h_i(x_j,y_j,z_j,t)=\Re e\left[h_{0_i}(x_j,y_j,z_j)e^{\imath\omega t}\right] \tag{13}$$

In eq. (13), the index j is the number of element and the index i is the normal mode number.

Using the same idea, in order to calculate the previously mentioned longitudinal derivatives, seven harmonic rigid body (quasy-steady or steady) motions of the general configuration, instead of normal modes, have to be incorporated:

B1. Quasi-steady harmonic change of the angle of attack

In developed software $\alpha_0=0.1$ is the default value, as it is acceptable in the used linear theories.

– On lifting surface j-th element in point (x,y,z)

$$h_{0_1}(x,y,z)=tg\alpha_0\left(x_{cg}-x\right)\cos\gamma_j;\ \frac{\partial h_{0_1}}{\partial x}=-tg\alpha_0\cos\gamma_j$$

Variable γ_j is dihedral angle of j-th lifting surface element.

– On image body axis j-th element in midpoint (x,y,z) in vertical direction

$$h_{0_1}(x,y,z)=tg\alpha_0\left(x_{cg}-x\right);\ \frac{\partial h_{0_1}}{\partial x}=-tg\alpha_0$$

B2. Steady pitch and quasi-steady harmonic vertical translation

In developed software $\frac{ql_{mac}}{2U}=0.1$ and $\bar{h}_z=0.1\frac{l_{\mathrm{ma}c}}{2}$ are default values, as they are acceptable in the used linear theories.

– For steady pitch on lifting surface j-th element in point (x,y,z), it follows

$$h_{0_2}(x,y,z)=0.1\frac{\left(x-x_{cg}\right)^2}{l_{mac}}\cos\gamma_j;\ \frac{\partial h_{0_2}}{\partial x}=0.2\frac{x-x_{cg}}{l_{mac}}\cos\gamma_j$$

On lifting surface j-th element in point (x,y,z) in quasi-steady harmonic vertical translation

$$h_{0_2}(x,y,z)=-\bar{h}_z\cos\gamma_j;\ \frac{\partial h_{0_2}}{\partial x}=0$$

– On image body axis j-th element in midpoint (x,y,z) in vertical direction for steady pitch, it follows:

$$h_{0_1}(x,y,z)=-0.1\frac{\left(x-x_{cg}\right)^2}{l_{mac}};\ \frac{\partial h_{0_1}}{\partial x}=0.2\frac{x-x_{cg}}{l_{mac}}$$

On image body axis j-th element in point (x,y,z) in quasi-steady harmonic vertical translation in vertical direction

$$h_{0_2}(x,y,z)=-\bar{h}_z;\ \frac{\partial h_{0_2}}{\partial x}=0$$

B3. Steady slat's deflection

The default slat deflection is $\delta_{slat}=0.1$. Only lifting surface elements on the wing's slats are deflected. In any slat control point (x_{kj},y_{kj},z_{kj}), it follows:

$$h_{0_3}=\delta_{slat}\left(x_{kj}-x^{arm}_{k,slot}\right)\cos\lambda_{slat};\ \frac{\partial h_{0_3}}{\partial x}=\delta_{slat}\cos\lambda_{slat}$$

In the above relations, $x^{arm}_{k,slot}$ is distance from control point to slat rotation axis and λ_{slat} is the swept angle of slat rotation axis. On all the other elements, meaning on all the other lifting surface elements and image bodies elements $h_{0_3}=0$ and $\frac{\partial h_{0_3}}{\partial x}=0$.

B4. Steady flap's deflection

The default flap deflection is $\delta_{flap}=0.1$. Only lifting surface elements on the wing's flaps are deflected. In any flap control point (x_{kj},y_{kj},z_{kj}) it follows:

$$h_{0_4}=\delta_{flap}\left(x_{kj}-x^{arm}_{k,flap}\right)\cos\lambda_{flap};\ \frac{\partial h_{0_4}}{\partial x}=\delta_{flap}\cos\lambda_{falp}\quad(14)$$

In eq. (14), $x^{arm}_{k,flap}$ is the distance from control point to flap rotation axis and λ_{flap} is the swept angle of flap rotation axis. On all the other elements, meaning on all the other lifting surface elements and image bodies elements $h_{0_4}=0$ and $\frac{\partial h_{0_4}}{\partial x}=0$.

B5. Steady symmetric aileron's deflection

If ailerons have different up and down deflection angles, any combination of their deflections can be obtained as the sum of symmetrical and antisymmetrical deflections.

$$\delta^{symm}_{ail}=\frac{1}{2}\left(\delta^{down}_{ail;}+\delta^{up}_{ail}\right);\ \delta^{anti}_{ail}=\frac{1}{2}\left(\delta^{down}_{ail}-\delta^{up}_{ail}\right)$$

The default symmetric aileron deflection is $\delta^{symm}_{ail}=0.1$. Only lifting surface elements on wing's ailerons are deflected. In any aileron control point (x_{kj},y_{kj},z_{kj}) it follows:

$$h_{0_5}=\delta^{symm}_{ail}\left(x_{kj}-x^{arm}_{k,ail}\right)\cos\lambda_{ail};\ \frac{\partial h_{0_5}}{\partial x}=\delta^{symm}_{ail}\cos\lambda_{ail}$$

In the above relations, $x^{arm}_{k,ail}$ is the distance from control point to aileron rotation axis and λ_{ail} is the swept angle of aileron rotation axis. On all the other elements, meaning on all the other lifting surface elements and image bodies elements $h_{0_5}=0$ and $\frac{\partial h_{0_5}}{\partial x}=0$.

B6. Steady elevator's deflection

The default symmetric elevator deflection is $\delta_{elev}=0.1$. Only lifting surface elements on the tail's elevator are deflected. In any elevator control point (x_{kj},y_{kj},z_{kj}) it follows:

$$h_{0_6}=\delta_{elev}\left(x_{kj}-x^{arm}_{k,elev}\right)\cos\lambda_{elev};\ \frac{\partial h_{0_6}}{\partial x}=\delta_{elev}\cos\lambda_{elev}\quad(15)$$

In eq. (15), $x^{arm}_{k,elev}$ is the distance from control point to flap rotation axis and λ_{elev} is the swept angle of elevator rotational axis. On all the other elements, meaning on all the other lifting surface elements and image bodies elements $h_{0_6}=0$ and $\frac{\partial h_{0_6}}{\partial x}=0$.

B7. Steady symmetric rudder's deflection

If aircraft's fin is out of configuration symmetry plane then steady aerodynamic derivatives for rudder symmetric deflection can be obtained. Usually in this case general configuration incorporates two fins out of aircraft's symmetry plane. The default symmetric rudder deflection is $\delta^{symm}_{rudd}=0.1$. Only lifting surface elements on the fins' rudders are deflected. In any rudder control point (x_{kj},y_{kj},z_{kj}) it follows:

$$h_{0_7}=\delta^{symm}_{rudd}\left(x_{kj}-x^{arm}_{k,rudd}\right)\cos\delta_{rudd};\ \frac{\partial h_{0_7}}{\partial x}=\delta^{symm}_{rudd}\cos\lambda_{rudd}$$

In the above relations, $x^{arm}_{k,rudd}$ is the distance from control point to rudder rotation axis and λ_{rudd} is the swept angle of rudder rotation axis. On all the other elements, meaning on

all the other lifting surface elements and image bodies elements $h_{0_7} = 0$ and $\frac{\partial h_{0_7}}{\partial x} = 0$.

Substituting (9) and (10) into (8) the following can be obtained:

$$\begin{aligned} \bar{C}_z &= \alpha_0 \left[C_{z\alpha} + \imath k \left(C_{z\dot{\alpha}} + C_{zq} \right) \right]; \\ \bar{C}_m &= \alpha_0 \left[C_{m\alpha} + \imath k \left(C_{m\dot{\alpha}} + C_{mq} \right) \right] \end{aligned} \tag{16}$$

Taking $\Im m\left(\bar{C}_z\right)$ and $\Im m\left(\bar{C}_m\right)$ from relations (16) it follows:

$$C_{z\dot{\alpha}} = \frac{1}{k} \Im m \frac{\bar{C}_z}{\alpha_0} - C_{zq}\,;\; C_{m\dot{\alpha}} = \frac{1}{k} \Im m \frac{\bar{C}_m}{\alpha_0} - C_{mq}$$

Steady longitudinal derivatives $C_{z\alpha}$, $C_{m\alpha}$, C_{zq} and C_{mq} can be determined from all over configuration's aerodynamic loadings integration in steady flow condition $(k = 0)$ by introducing (9) and (10) into (13).

In order to account unsteady longitudinal derivatives $C_{z\ddot{\alpha}}$ and $C_{m\ddot{\alpha}}$, it is necessary to introduce (11) into (8). Then:

$$\begin{aligned} \frac{\bar{C}_z}{h_z / l_{mac}} &= \imath k C_{z\alpha} - k^2 C_{z\dot{\alpha}} - \imath k^3 C_{z\ddot{\alpha}}; \\ \frac{\bar{C}_m}{h_z / l_{mac}} &= \imath k C_{m\alpha} - k^2 C_{m\dot{\alpha}} - \imath k^3 C_{m\ddot{\alpha}} \end{aligned} \tag{17}$$

Taking $\Im m\left(\bar{C}_z\right)$ and $\Im m\left(\bar{C}_m\right)$ from relations (17) it can be obtained:

$$C_{z\ddot{\alpha}} = \frac{1}{k^3} \left[\Im m \left(\frac{\bar{C}_z}{h_z / l_{mac}} + k^2 C_{z\dot{\alpha}} \right) + k C_{z\alpha} \right];$$

$$C_{m\ddot{\alpha}} = \frac{1}{k^3} \left[\Im m \left(\frac{\bar{C}_m}{h_z / l_{mac}} + k^2 C_{m\dot{\alpha}} \right) + k C_{m\alpha} \right];$$

For determination of unsteady derivatives, it is necessary to develop (6) and (7) in the Mac Laurent series of higher order and it follows:

$$\begin{aligned} \bar{C}_z &= \alpha_0 \left[C_{z\alpha} + \imath k \left(C_{z\dot{\alpha}} + C_{zq} \right) - k^2 \left(C_{z\ddot{\alpha}} - C_{z\dot{q}} \right) \right] \\ \bar{C}_m &= \alpha_0 \left[C_{m\alpha} + \imath k \left(C_{m\dot{\alpha}} + C_{mq} \right) - k^2 \left(C_{m\ddot{\alpha}} - C_{m\dot{q}} \right) \right] \end{aligned} \tag{18}$$

In (18) only $C_{z\dot{q}}$ and $C_{m\dot{q}}$ are unknown. So, taking $\Re e(\bar{C}_z)$ and $\Re e(\bar{C}_m)$ from (18) it can be found:

$$C_{z\dot{q}} = -C_{z\ddot{\alpha}} - \frac{1}{k^2} \left\{ C_{z\alpha} - \Re e \left[\frac{\bar{C}_z}{\alpha_0} - \imath k \left(C_{z\dot{\alpha}} + C_{zq} \right) \right] \right\}$$

$$C_{m\dot{q}} = -C_{m\ddot{\alpha}} - \frac{1}{k^2} \left\{ C_{m\alpha} - \Re e \left[\frac{\bar{C}_m}{\alpha_0} - \imath k \left(C_{m\dot{\alpha}} + C_{mq} \right) \right] \right\}$$

Examples

Two examples from the well known software NASTRAN are tested. The first example was case HA21A for steady longitudinal aerodynamic derivatives, and the second was the case HA75H for unsteady flow.

Case HA21A

The case is taken from [3]. Forward-Swept-Wing (FSW) airplane with coplanar canard-wing configuration was tested in the trimmed sea level steady flight at Mach 0.9. The model is idealized as shown on Fig.5.

The wing has an aspect ratio 4.0, no taper, twist, camber, or incidence relative to fuselage, and a forward sweep angle of 30^o. The canard has an aspect ratio 1.0, and no taper, twist, camber, incidence, or sweep. The chords of both the wing and canard are $3050,00$ [mm], and reference length is equal to the wing mid aerodynamic chord $l_{mac} = 3050,00$ [mm]. The half-span model of aircraft is divided in 32 equal panels (8 span-wise, 4 chord-wise) on the wing and 8 equal panels (2 span-wise, 4 chord-wise) on the canard. The fuselage length is $9150,00$ [mm]. Aerodynamic forces on the fuselage are neglected.

The aerodynamic coordinate system is located in the beginning of the fuselage in coplanar plane of wing-canard configuration. Center of gravity is $4575,00$ [mm] behind aerodynamic coordinate system origin in mid point of canard root-chord.

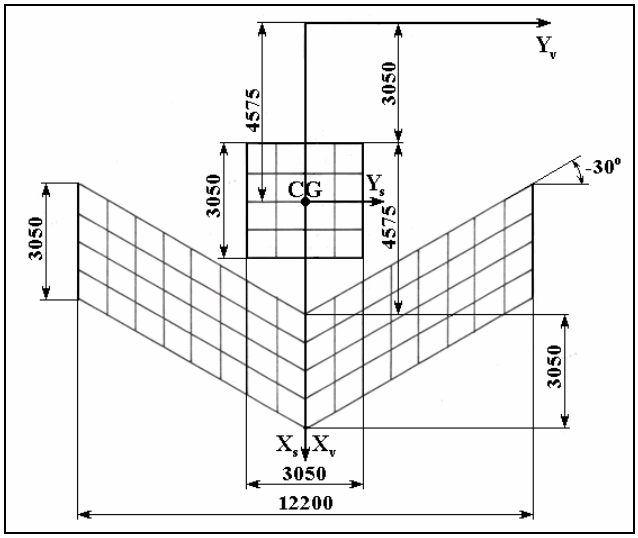

Figure 5. The example HA21A idealization

The comparison of results from [3] and DERIV are given in Table 1. Steady derivatives $C_{z\delta_c}$ and $C_{m\delta_c}$ are related to canard deflection δ_c.

Table 1. Comparison of the results for the example HA21A

Software	$C_{z\alpha}$	$C_{m\alpha}$	C_{zq}	C_{mq}	$C_{z\delta_c}$	$C_{m\delta_c}$
NASTRAN [3]	-5.0711	-2.8712	-12.0746	-9.9549	-0.2461	0.5715
DERIV	-5.0710	-2.8710	-12.0740	-9.9540	-0.2461	0.5715

Based on the results given in Table 1, steady longitudinal aerodynamic derivatives from NASTRAN and DERIV are in good agreement.

Case HA75H

The case is taken from [5] and [6], and its geometry form NASTRAN. Typical transport aircraft's wing was tested in unsteady flow at Mach 0.8 at the sea level. Geometry of the wing is given on Fig.6. The wing has an aspect ratio

8.0, taper $l_{tip}/l_{root} = 0.25$, no twist, camber, or incidence relative to fuselage, and the leading edge sweep angle of 33.1142°. The sweep angle of the wing mean aerodynamic chords' line is 30°. The pitch axis of the wing includes point at $l_{mac}/4$. In the wing's symmetry plane origin of pitch axis is at 827.35 [mm] behind the leading edge of the wing's root chord. The half-span model of wing is divided in 75 panels (15 equal span-wise, 5 equal chord-wise).

In [6] and DERIV moments' derivatives are calculated for pitch axis located in wing symmetry's plane at $l_{mac}/4$. As in [5] pitch axis was in leading wing edge in its symmetry plane, it was necessary to recalculate moments' derivatives. If $(C_{m*})_1$ and $(C_{m*})_2$ are moments' derivatives for longitudinal location of pitch axis x_1 and x_2, respectively, then they are correlated using relation:

$$(C_{m*})_2 = (C_{m*})_1 + C_{z*}\frac{x_1 - x_2}{l_{mac}}$$

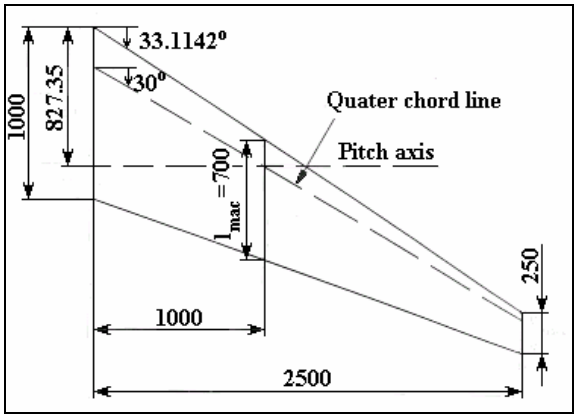

Figure 6. The example HA21H idealization

In the Table 2 calculated steady and unsteady longitudinal aerodynamic derivatives are given, taken from [5], [6] and DERIV. Unsteady derivatives are compared for reduced frequency $k = \omega l_{mac}/(2U) = 0.010$. The data marked as (*) in the Table 2 is not represented in [5] or [6].

Table 2. Comparison of the results for the example HA75H

	[5]	[6]	DERIV
$C_{m\alpha}$	(*)	- 5.8490	- 5.8455
$C_{m\alpha}$	(*)	- 0.5643	- 0.5847
C_{zq}	(*)	- 5.9360	- 5.9978
C_{mq}	(*)	- 3.2050	- 3.2887
$C_{z\dot{\alpha}}$	12.5300	12.5400	12.4325
$C_{m\dot{\alpha}}$	0.8504	0.8744	0.8980
$C_{m\dot{q}}$	-16.4000	(*)	-16.3317
$C_{m\dot{q}}$	(*)	(*)	0.7749
$C_{z\ddot{\alpha}}$	94.7000	(*)	93.7748
$C_{m\ddot{\alpha}}$	11.6375	(*)	11.1347

Based on the Table 2, the results for HA75H obtained from [5], [6] and DERIV are in good agreement.

Conclusion

A concise overview of the developed numerical procedure and test results of new software DERIV, for calculation of longitudinal aerodynamic derivatives for general configurations, are given in the paper.

The contributions of the research given can be seen in the detailed numerical development of the selected method and in the development and testing of the software DERIV.

The developed software DERIV is tested through NASTRAN cases HA21A and HA75H. The obtained results for DERIV are in good agreement to NASTRAN, [5] and [6].

In the future, DERIV software ought to be tested in cases from the engineering practice.

References

[1] ETKIN,B.: *Dynamics of flight*, Wiley, New York, 1959.

[2] GIESING,J., KALMAN,T., RODDEN,W.: *Subsonic Unsteady Aerodynamics for General Configurations*, Part II, Vol.I, Wright-Patterson Air Force Dynamic Laboratory, Tech.Rep. AFFDL-TR-71-5, Ohio, April 1972.

[3] BELLINGER,E.: *MSC/NASTRAN Aeroelastic Supplement*, The Mac Neal Schwendler Corporation, Los Angeles, June 1986.

[4] MARIČIĆ,N.: *Contribution to calculation of aircraft's critical flutter speeds*, PhD dissertation, Faculty of Mechanical engineering, Belgrade, January 1990. (in Serbian)

[5] RODDEN,W., GEISING,J.: *Application of Oscillatory Aerodynamic Theory to Estimation of Dynamic Stability Derivatives*, J.Aircraft, May-June, 1970, Vol.7, No.3

[6] RODDEN,W., BELLINGER,E., GEISING,J.: *Errata and Addenda to "Application of Oscillatory Aerodynamic Theory to Estimation of Dynamic Stability Derivatives*, J.Aircraft, January, 1984, Vol.21, No.1

[7] MSC Software Corp. NEWPAN - MSC. NASTRAN™ AEROELASTIC, 2004.

Received: 15.04.2005.

Razvoj softvera za proračun uzdužnih aerodinamičkih derivativa podzvučnih aviona

Uzdužni aerodinamički derivativi subsoničnih aviona proizvoljne konfiguracije mogu se izračunati (proceniti) korišćenjem metoda konačnih elemenata baziranih na metodi rešetke dubleta (Doublet Lattice Method - DLM), teoriji vitkih tela (Slender Body Theory -- SBT) i metodi zamena (Method of Images -- MI). Primenom navedene metodologije razvijen je softverski paket DERIV. Rezultati dobijeni programom DERIV testirani su na primerima HA21A i HA75H iz NASTRAN-a. Postignuto je dobro slaganje rezultata iz DERIV-a, NASTRANA-a, [5] i [6].

Ključne reči: **aerodinamika, nestacionarna aerodinamika, aerodinamički derivativi, uzdužna stabilnost, podzvučni avion.**

Le développement du logiciel pour calculer les dérivatifs longitudinaux aérodynamiques non-stationnaires des avions subsoniques

Les dérivatifs longitudinaux aérodynamiques non-stationnaires des avions subsoniques de configuration arbitraire peuvent etre calculés par l'application de la méthode des éléments finis basés sur la méthode de grille des doublets (Doublet Lattice Method-DLM), théorie des corps élancés (Slender Body Theory-SBT) et méthode de substitutions (Method of Images-MI).En appliquant la méthodologie citée on a développé un progiciel DERIV.Les résultats obtenus par le programme DERIV ont été testé sur les exemples HA 21A et HA75H de NASTRAN.Un bon accord a été réalisé entre les résultats obtenus par DERIV et par NASTRAN de [5] et [6].

Mots clés: **aérodynamique, aérodynamique non-stationnaire, dérivatifs aérodynamiques, stabilité longitudinale, avions subsoniques.**

Развитие программного обеспечения для неустойчивых, продольных аэродинамических деривативов дозвуковых самолётов

Неустойчивые, продольные аэродинамические деривативы дозвуковых самолётов произвольной компоновочной схемы могут быть высчитаны - оценены пользованием метода конечных элементов которые базируются на методе решётки дублетов, на теории гибких тел и на методе замещения. Применением приведённой методологии развился новый пакет программного обеспечения DERIV. Результаты полученые программой DERIV сравниваны с образцами HA21A и HA75H из программы NASTRAN. Достигнуто хорошее согласование результатов.

Ключевые слова: **аэродинамика, неустойчивая аэродинамика, аэродинамические деривативы, продольная устойчивость, дозвуковой самолёт.**